Cerebral injury in perinatally HIV-infected children compared to matched healthy controls

Sophie Cohen, MD
Matthan W.A. Caan, PhD
Henk-Jan Mutsaerts, MD
Henriette J. Scherpbier, MD, PhD
Taco W. Kuijpers, MD, PhD
Peter Reiss, MD, PhD
Charles B.L.M. Majoie, MD, PhD
Dasja Pajkrt, MD, PhD

Correspondence to Dr. Cohen: s.cohen@amc.nl

ABSTRACT

Objective: The current study aims to evaluate the neurologic state of perinatally HIV-infected children on combination antiretroviral therapy and to attain a better insight into the pathogenesis of their persistent neurologic and cognitive deficits.

Methods: We included perinatally HIV-infected children between 8 and 18 years and healthy controls matched for age, sex, ethnicity, and socioeconomic status. All participants underwent a 3.0 T MRI with 3D-T1-weighted, 3D-fluid-attenuated inversion recovery, and diffusion-weighted series for the evaluation of cerebral volumes, white matter hyperintensities (WMH), and white matter (WM) diffusion characteristics. Associations with disease-related parameters and cognitive performance were explored using linear regression models.

Results: We included 35 cases (median age 13.8 years) and 37 controls (median age 12.1 years). A lower gray matter and WM volume, more WMH, and a higher WM diffusivity were observed in the cases. Within the HIV-infected children, a poorer clinical, immunologic, and virologic state were negatively associated with volumetric, WMH, and diffusivity markers.

Conclusions: In children with HIV, even when long-term clinically and virologically controlled, we found lower brain volumes, a higher WMH load, and poorer WM integrity compared to matched controls. These differences occur in the context of a poor cognitive performance in the HIV-infected group, and larger, longitudinal studies are needed to increase our understanding of the pathogenesis of cerebral injury in perinatally HIV-infected children. ***Neurology*® 2016;86:19–27**

GLOSSARY

cART = combination antiretroviral therapy; **CDC** = Centers for Disease Control and Prevention; **DTI** = diffusion tensor imaging; **DWI** = diffusion-weighted image; **FA** = fractional anisotropy; **FLAIR** = fluid-attenuated inversion recovery; **FOV** = field of view; **GM** = gray matter; **ICV** = intracranial volume; **MD** = mean diffusivity; **NPA** = neuropsychological assessment; **RD** = radial diffusivity; **SES** = socioeconomic status; **TBSS** = tract-based spatial statistics; **TE** = echo time; **TI** = inversion time; **TR** = repetition time; **WM** = white matter; **WMH** = white matter hyperintensities.

Despite the decline in incidence of neurologic complications such as HIV encephalopathy since the introduction of combination antiretroviral therapy (cART), perinatally HIV-infected children present with neurologic and cognitive deficits.[1]

MRI studies have detected cortical atrophy, white matter hyperintensities (WMH), and basal ganglia calcifications in HIV-infected adults, including in those with suppressed viremia on treatment.[2,3] Pre-cART neuroimaging studies in children showed comparable cerebral abnormalities; however, MRI studies in perinatally HIV-infected children using cART are scarce.[4,5] One study detected no cortical atrophy, and white matter (WM) atrophy only in specific areas such as the corpus callosum and external capsule.[6] Another found WMH in 50% of children; however, all had suspected HIV-related brain disease.[7] Finally, one study detected poor WM integrity in HIV-infected children, analogous to adults, but these children were all cART-naive with slow disease progression.[8]

Editorial, page 13

Supplemental data at Neurology.org

From the Department of Pediatric Hematology, Immunology and Infectious Diseases (S.C., H.J.S., T.W.K., D.P.), Emma Children's Hospital AMC, Amsterdam; the Department of Radiology (M.W.A.C., H.-J.M., C.B.L.M.M.), the Department of Global Health and Amsterdam Institute of Global Health and Development (P.R.), and the Department of Internal Medicine, Division of Infectious Diseases, Center for Infection and Immunity Amsterdam (CINIMA) (P.R.), Academic Medical Centre, University of Amsterdam; and HIV Monitoring Foundation (P.R.), Amsterdam, the Netherlands.

Go to Neurology.org for full disclosures. Funding information and disclosures deemed relevant by the authors, if any, are provided at the end of the article.

These findings are thought to be caused by various pathophysiologic mechanisms, including early HIV-related damage, ongoing immune activation, and cART toxicity.[9] In perinatally HIV-infected children, CNS invasion of HIV occurs in the first 3 weeks of life,[9] which is among the most important reasons why research concerning their persistent neurologic problems is essential. However, studies investigating these mechanisms in relation to imaging and cognitive parameters, particularly in perinatally HIV-infected children, are limited.

Recently, we found poorer cognitive performance in a study comparing perinatally HIV-infected children to age-, sex-, ethnicity- and socioeconomically matched healthy controls.[10] The current study focuses on MRI differences among these groups and explores the potential pathophysiologic mechanisms underlying them.

METHODS

Standard protocol approvals, registrations, and patient consents. The ethics committee of the Academic Medical Center approved the study protocol. Informed consent was obtained from parents and children age 12 years and older.

Participants. From December 2012 until January 2014, we approached all perinatally HIV-infected patients between 8 and 18 years of age attending our outpatient clinic. Controls were recruited as described previously.[10] We determined the HIV status of controls by the Diasorin Liaison HIV-1-antigen/antibody test. Exclusion criteria were chronic (non-HIV-associated) neurologic diseases such as seizure disorders, (history of) intracerebral neoplasms, traumatic brain injury, psychiatric disorders, and MRI contraindications (metal implants or claustrophobia).

Controls were matched for age, sex, ethnicity, and socioeconomic status (SES). Matching for SES, determined using parental educational level and occupational status, was done to account for its effect on cognitive performance.[11] Parental education was scored according to the International Standard Classification of Education. Disease- and therapy-related parameters were collected from the Dutch HIV monitoring foundation database (www.hiv-monitoring.nl). A full description of these parameters was published previously.[10]

MRI data acquisition. All images were acquired on a 3.0 T MRI scanner (Intera, Philips Healthcare, Best, the Netherlands) equipped with a 16-channel phased array head coil. Head motion was restricted with foamed material inside the coil. A neuroradiologist examined all images for coincidental findings, and detected 1 HIV-infected patient with an Arnold-Chiari malformation, and 1 control with a retrocerebellar cyst. As these were minor conditions, these children were not excluded. Structural 3D T1-weighted images were acquired using magnetization-prepared rapid acquisition gradient echo (repetition time [TR] 7.0 ms; echo time [TE] 3.18 ms; inversion time [TI] 900 ms; flip angle 9°; field of view [FOV] 256 mm × 256 mm^2; 180 slices). Three-dimensional fluid-attenuated inversion recovery (FLAIR) visualized WMH in periventricular and deep WM (TR/TE 4,800/356 ms; TI 1,650 ms; FOV 240 × 240 mm^2; 321 over-contiguous sagittal slices of 0.56 mm thickness; 1 × 1 mm^2 in-plane resolution). Diffusion tensor imaging (DTI) parameters were acquired using spin echo single shot echoplanar imaging along 64 directions with b = 1,000 seconds/mm^2 and 4 averages with b = 0 seconds/mm^2 (TR 9,476 ms, TE 92 ms, FOV 224 × 224 mm, voxel size 2.0 mm^3 isotropic).

MRI data processing. Data were anonymized prior to analysis. Processing was performed using in-house developed software, written in Matlab (The MathWorks, Natick, MA), and was executed on the Dutch Grid, using a Web interface to the e-Bioinfra gateway.[12] T1-weighted images were segmented using Freesurfer Image Analysis suite v5.0.[13] All segmentation inaccuracies were checked manually. Participants with excessive head movements were excluded.

FLAIR images were processed using a semiautomatic technique. After bias-field correction, a mask (mask 1) for WMH was created by intensity thresholding using individually determined intensity thresholds on the level of the quadrigeminal plate. A second mask (mask 2) was created by manual gross contouring of WMH. The final mask (intersection of mask 1 and 2) was created using FSLmaths, manually inspected, and corrected to serve as the WMH map for volume calculation.

For DTI images, head motion and deformations induced by eddy currents were corrected for by an affine registration of the diffusion-weighted images (DWIs) to the non-diffusion-weighted image. Gradient directions were corrected by the rotation component of the transformation. The DWIs were resampled isotropically. Rician noise in DWIs was reduced by an adaptive noise filtering method.[14] Diffusion tensors were estimated in a nonlinear least squares sense. From the tensors, fractional anisotropy (FA), mean diffusivity (MD), axial diffusivity, and radial diffusivity (RD) maps were computed. Whole brain WM averaged DTI measures were computed by averaging over the entire skeleton.

A voxel-wise statistical analysis of the DTI data was performed using tract-based spatial statistics (TBSS) implemented in the FMRIB Software Library 4.1.6 (University of Oxford, UK).[15] FA data were aligned into a common space using the nonlinear registration tool FNIRT, which uses a b-spline representation of the registration warp field.[16] The mean FA image was created and thinned to create a mean FA skeleton, representing the centers of all tracts common to the group. Each subject's aligned FA data were then projected onto this skeleton and the resulting data fed into voxel-wise cross-subject statistics.

We pairwise assessed group differences for FA, axial diffusivity, RD, and MD using age, sex, and intracranial volume (ICV) as covariates by means of Randomise, a TBSS statistical tool that computes nonparametric permutations using the generalized linear model. We reported significant values at $p < 0.05$, using threshold-free cluster enhancement.[17] The number of permutations was set to 500. The principal WM tracts were identified in the John Hopkins University WM probabilistic tractography and ICBM WM label atlases.[18]

Neuropsychological assessment. On the same day as the MRI scan, participants underwent a comprehensive neuropsychological assessment (NPA) evaluating intelligence, information processing speed, attention, memory, executive function, and visual-motor function. A description of the methods and results of this NPA was previously published.[10]

Statistical analysis. Data entry and management was performed using OpenClinica software. Statistical analyses were

Table 1 Participant characteristics

	HIV-infected (n = 31)	Healthy (n = 37)	p Value
Demographic characteristics			
Male sex	16 (52)	18 (49)	0.808
Age at MRI	13.4 (11.4–15.9)	12.1 (11.5–15.9)	0.263
Ethnicity			0.405
Black	25 (81)	28 (76)	
Mixed black	4 (13)	6 (16)	
Caucasian	0 (0)	3 (8)	
Other	2 (6)	0 (0)	
Country of birth			<0.001[a]
Netherlands	11 (36)	35 (95)	
Sub Saharan Africa	15 (48)	2 (5)	
Suriname	2 (6)	0 (0)	
Other	3 (10)	0 (0)	
Age arrived in the Netherlands, y	0.8 (0–4.7)	0 (0–0)	<0.001[a]
Care setting			0.762
One parent	22 (63)	25 (68)	
Two parents	9 (29)	12 (32)	
Adoption			0.002[a]
Not adopted	25 (71)	37 (100)	
Adopted	3 (10)	0 (0)	
Foster care	6 (19)	0 (0)	
Education			0.035[a]
Primary school	9 (29)	19 (51)	
High school	13 (32)	14 (38)	
Special school	7 (23)	1 (3)	
Other	5 (16)	3 (8)	
Country of birth, mother/father			<0.001[a]
Netherlands	1 (3)/4 (13)	6 (16)/8 (22)	
Sub-Saharan Africa	23 (74)/16 (52)	8 (22)/5 (14)	
Suriname	3 (10)/4 (13)	19 (51)/20 (54)	
Other	4 (13)/5 (16)	4 (11)/4 (11)	
Parental marital status			0.706
Married	7 (23)	9 (24)	
Divorced or single	24 (77)	27 (73)	
Other	2 (6)	1 (3)	
ISCED educational level[b]	5 (4–6)	5 (5–6)	0.791
One parent employed	16 (53)	25 (68)	0.234
Two parents employed	4 (15)	9 (24)	0.388
HIV- and cART-related characteristics			
Clinical			
Age at HIV diagnosis, y	1.2 (0.6–4.9)	—	—
CDC category		—	—
N	4 (13)	—	—
A	5 (16)	—	—

Continued

carried out using Stata, v12 (StataCorp LP, College Station, TX). Demographic characteristics were compared between groups using the unpaired *t* test or the Mann-Whitney *U* test and the χ^2 test. Values of brain volumes, WMH, and DTI parameters were compared between groups using regression analyses adjusted for sex, age, and ICV, and additionally for total gray matter (GM) in the WMH model as there is a known association between cortical volume and WMH.[19] Effect sizes were calculated by dividing the difference in mean scores between both groups by their pooled SD.

Associations between disease-related parameters and MRI results (total GM and WM volume, MD, and FA) were investigated using multivariable linear regression models adjusted for age and sex. Volumetric outcomes were additionally adjusted for ICV. We explored associations between MRI parameters and those neuropsychological domains most impaired in the HIV-infected group (total IQ, processing speed index, and attention span)[10] using linear regression models adjusted for age.

RESULTS

Participants. In total, 35 HIV-infected and 37 matched healthy children were included. Four HIV-infected children were excluded from MRI examination due to dental braces or claustrophobia. Demographic and disease-related characteristics are shown in table 1. None of the study participants had depression, used antidepressants, or received any other psychiatric treatment. None of the controls had a positive HIV test.

Two HIV-infected children were diagnosed previously with HIV encephalopathy, and 1 with cytomegalovirus encephalitis. The latter was excluded from all analyses. Twenty-eight children (90%) were on cART at inclusion, 27 of whom had suppressed viremia (94%). Two children had stopped therapy for personal reasons within 6 months before inclusion, and 1 child had never been on cART. The latter was not excluded; however, a sensitivity analysis without the cART-naive child did not alter the results (data not shown). HIV-infected children were infected with a variety of HIV subtypes (table e-1 on the *Neurology*® Web site at Neurology.org).

Volumetric analysis. The HIV-infected group had lower cortical and total GM volume and a lower WM volume (table 2). We observed a trend between WM volume and age (coefficient = 3.5, $p = 0.112$), which was predominantly driven by an association in controls (coefficient = 6.16; $p = 0.037$), but not in cases (coefficient = 2.1; $p = 0.529$). We found no specific regions where GM or WM volume differences were more pronounced.

White matter lesions. WMH were seen in 16 cases (59%, mean volume: 2.2 log cm^3, SD 0.7, range 1.2–3.9) and 6 controls (18%, mean volume: 2.0 log cm^3, SD 0.3, range 1.5–3.9) ($p < 0.001$). WMH were found in both the juxtacortical and deep WM, and were not detected in specific cerebral lobes (figure 1).

Table 1 Continued

	HIV-infected (n = 31)	Healthy (n = 37)	p Value
B	13 (42)	—	—
C	9 (29)		
Cerebral HIV/AIDS	3 (10)[c]	—	—
CD4+ T cells and HIV viral load			
Peak HIV viral load (log copies/mL)	5.5 (5.1–5.9)	—	—
Nadir CD4+ *Z* score	−0.7 (−1.5 to 0.4)	—	—
HIV viral load at MRI		—	—
Detectable	4 (13)	—	—
Undetectable	27 (87)		
CD4+ T-cell count at MRI ($\times 10^6$/L)	800 (590–1,030)	—	—
Time living with a detectable viral load, y	2.8 (1.4–6.4)	—	—
Time living with CD4+ T-cell count <500 ($\times 10^6$/L), y	0.6 (0.4–3.1)	—	—
cART			
Age at cART initiation, y	2.2 (0.9–5.2)	—	—
Current cART use	28 (90)	—	—
Duration cART use, y	11.8 (7.7–14.5)	—	—
Monotherapy or dual therapy treatment before cART	3 (10)	—	—
MRIs of good quality for assessment[d]			
MPRAGE	27 (87)	37 (100)	—
FLAIR	26 (84)	34 (92)	—
DTI	28 (90)	36 (97)	—

Abbreviations: cART = combination antiretroviral therapy; CDC = Centers for Disease Control and Prevention; DTI = diffusion tensor imaging; FLAIR = fluid-attenuated inversion recovery; ISCED = International Standard Classification of Education; MPRAGE = magnetization-prepared rapid acquisition gradient echo.
Values are n (%) or median (IQR).
[a] $p < 0.05$.
[b] Most educated parent.
[c] HIV encephalopathy n = 2 and cytomegalovirus encephalitis n = 1.
[d] There were no significant differences in any demographic, HIV, or cART-related parameters between children in whom analysis could be performed vs children in whom analysis could not be performed.

White matter microstructure. MD, RD, and axial diffusivity were higher (all $p \leq 0.001$) and FA was lower in cases ($p = 0.030$) (table 2). Masking out WMH did not alter these results.[20] Whole brain TBSS showed a higher MD, RD, and axial diffusivity in cases, with widespread effects throughout the brain (figure 2). With TBSS, no difference in FA was found ($p = 0.20$).

Associations with HIV and cART-related factors. Within the cases, we explored associations between disease-related factors and MRI parameters (table 3). A higher zenith HIV viral load was associated with a lower FA (coefficient −1.77, $p = 0.041$). A higher FA was associated with a higher nadir CD4 *Z* score (coefficient 1.29, $p = 0.033$). A longer time with low CD4+ T-cell counts was associated with a lower total GM volume (coefficient −12.73, $p = 0.014$). A poorer Centers for Disease Control and Prevention (CDC) clinical state (B or C) was associated with a lower total WM volume (CDC B: coefficient −48.42, $p = 0.006$; CDC C: coefficient −45.89, $p = 0.019$). No associations were found between HIV subtypes and MRI outcome parameters.

Associations with cognitive performance. In all study participants, GM and WM volumes were associated with a higher IQ (GM: coefficient 0.07, $p = 0.009$; WM: coefficient 0.11, $p = 0.002$). Higher MD was associated with lower IQ (coefficient −1.63, $p = 0.038$). Higher GM and WM volumes were associated with a better processing speed (GM: coefficient 0.06, $p = 0.020$; WM: coefficient 0.09, $p = 0.023$). MD was associated with a lower digit span (coefficient −0.38, $p = 0.021$) and increased FA was associated with a higher digit span (coefficient 0.34, $p = 0.025$) (table e-2).

In the HIV-infected group alone, coefficients were similar but associations were not significant, apart from the total WM volume and IQ (coefficient 0.11, $p = 0.029$) (table e-2 and figures e-1 and e-2).

DISCUSSION The current study detected a lower GM and WM volume, a higher WMH lesion load, and poorer WM integrity in otherwise well-controlled perinatally HIV-infected children, compared to controls. Early HIV-related CNS damage, as well as ongoing low-grade viral replication and immune activation, may be important elements of the pathophysiologic mechanism behind these findings. The observed cerebral injury was associated with poorer cognitive performance in multiple domains.[10]

MRI studies are scarce in cART-treated HIV-infected children.[4] Contrasting our results, one post-cART pediatric study on cerebral volumes detected no global GM or WM differences between HIV-infected youths and age-matched controls. The authors did observe WM atrophy in specific areas, such as the corpus callosum. In addition, they found a focal increase in GM, and carefully attributed it to cell swelling as a result of ongoing infection or cART toxicity.[6] We found no (focal) increase in either GM or WM.

The high prevalence of WMH in HIV-infected children in this study was similar to a previous South African pediatric study from the post-cART era. However, their patients were substantially younger (mean age 2.5 years) and underwent neuroimaging for suspected HIV-related neurologic disease.[7] We had anticipated a lower prevalence of WMH in our cases, who were without suspected

Table 2 Comparisons of regional brain volumes, DTI parameters, and WMH volumes between HIV-infected and healthy children

	HIV-infected		Healthy					
MRI sequence	Mean	SD	Mean	SD	Coefficient	95% CI	p Value[a]	ES
T1-weighted								
Total white matter	424	51	444	49	−175	−348 to-2	0.047	0.3
Cortical gray matter	182	17	194	14	−121	−182 to −60	<0.001	0.8
Total gray matter	667	58	700	75	−266	−517 to −16	0.037	0.5
CSF	1.34	0.41	1.21	0.20	1.31	−0.2 to 2	0.078	0.5
FLAIR								
WMH volumes	1.34	1.23	0.35	0.79	0.98	0.42 to 1.53	0.001	0.9
DTI								
FA	0.42	0.03	0.43	0.02	−0.01	−0.03 to −0.001	0.030	0.4
MD	0.79	0.03	0.77	0.02	0.25	0.15 to 0.36	<0.001	1.2
RD	0.60	0.03	0.57	0.03	0.27	0.13 to 0.41	<0.001	1
Axial diffusivity	1.19	0.03	1.17	0.02	0.22	0.10 to 0.35	0.001	0.8

Abbreviations: CI = confidence interval; DTI = diffusion tensor imaging; ES = effect sizes (small <0.2, medium 0.2–0.8, large >0.8); FA = fractional anisotropy; FLAIR = fluid-attenuated inversion recovery; MD = mean diffusivity; RD = radial diffusivity; WMH = white matter hyperintensity.
Mean/SD values for volumes and FLAIR measures in cm^3. MD/RD/axial diffusivity values are $\times 10^3$.
[a] The *p* values are adjusted for sex, age, and intracranial volume.

intracerebral HIV involvement. An explanation for this finding may be our stronger magnetic field strength of 3.0, since 1.5 T has a reduced sensitivity to subtle WMH.[21] In addition, WM myelination occurs mainly in the first 2 years of life and continues at least up to 5 years of age.[22] The majority of patients in the South African study thus had immature WM, which may have resulted in a different pattern of WMH than in our older patients. Nonetheless, WMH are generally thought to represent myelin loss, vasculopathy, and gliosis, partly due to ongoing immune activation.[9] WMH in perinatally HIV-infected children may therefore increase with age, which would support a higher lesion load in our cases.

The WMH diffusely affected juxtacortical and deep WM of the HIV-infected children, while the South African study observed WMH mainly in the frontal and parietal lobes.[7] Lesions in the juxtacortical WM are described in inflammatory conditions such as multiple sclerosis and have been associated with cognitive functioning.[23,24] They are less associated with perfusion problems as juxtacortical WM is thought to be better perfused than deeper WM.[25]

A notable finding was that WMH were also found in 18% of the controls. As described above, it is agreed upon that it is abnormal for WM to be hyperintense after the second year of life.[22] Thus far, the reported prevalence of WMH in healthy children or adolescents varies from 0% to 31%. Of note, these reports used a 1.5 T scanner and did not use FLAIR but an inferior T2-weighted sequence.[26,27] WMH increase with age, with a prevalence of 11%–21% in adults aged around 64 years to 94% at age 80 years.[26] The considerable proportion of controls with WMH and the variable prevalence in the existing literature warrants further investigation, but also suggests that including a control group was essential to not overestimate the occurrence of WMH in pediatric HIV.

Besides GM atrophy and WMH, HIV-infected patients had a higher MD and a lower FA, suggesting a poorer integrity of WM.[28] Increased axial diffusivity is usually associated with a better WM integrity; however, co-occurring with higher RD, it may represent simultaneous axonal and myelin degeneration. One previous pediatric study investigating cerebral diffusion characteristics of a group of cART-naive HIV-infected children with slow disease progression showed similar results.[8] In our study, TBSS analyses exposed a diffuse pattern of poorer WM integrity, analogous to adult HIV studies that reported a higher MD, RD, and axial diffusivity and a lower FA, generally in many cerebral regions.[29,30] The difference in FA was less pronounced than in the diffusivity markers. However, the increase of both axial diffusivity and RD in may have partially cancelled out a reduction in FA.[31]

Figure 1 Distribution of white matter hyperintensities

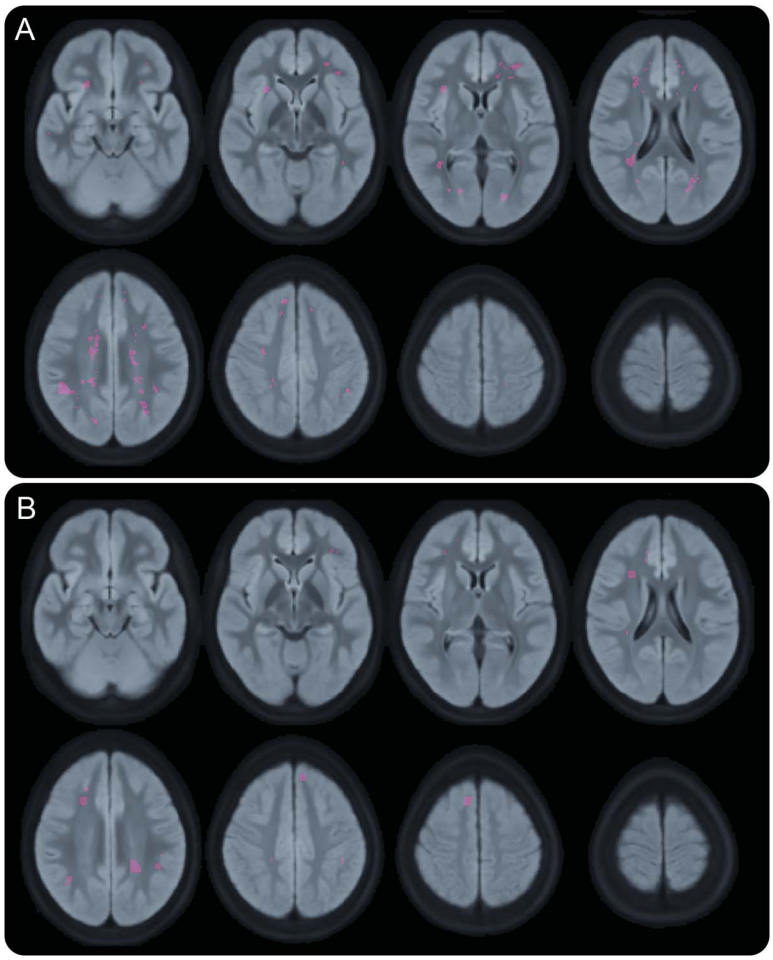

(A) HIV-infected children (n = 16, 59%; mean volume = 2.2 cm^3, SD = 0.7, range 1.2–3.9). (B) Healthy controls (n = 6, 18%; mean volume = 2.0 cm^3, SD = 0.3, range = 1.5–3.9).

Various pathophysiologic mechanisms could underlie the cerebral differences detected in this study. First, HIV-related brain damage inflicted before cART initiation may be irreversible. HIV predominantly infects perivascular macrophages and microglia cells in the CNS, which are thought to produce neurotoxic viral proteins and inflammatory mediators.[9] Associations among the zenith HIV VL, the nadir CD4+ T-cell *Z* score, and FA support this theory. Also, a poorer clinical state at diagnosis was associated with a lower WM volume in this study and with lower IQ reported previously.[10] The association between the time with a low CD4+ T-cell count and GM volume may indicate that prolonged immunosuppression plays an additional role in CNS damage. Thus, besides damage done before treatment, ongoing low-grade viral replication may also have adverse consequences for the CNS.[32] This is further illustrated by the lack of increase in WM volumes with age in the HIV-infected children, while it increased in their age-matched peers. However, the median age at cART initiation was approximately 2 years, which may be beyond the window of opportunity to prevent early damage in perinatally HIV-infected children. A pediatric DTI study showed that a higher HIV VL, a lower CD4+ T-cell count, and having started a second-line cART were all associated with poorer WM integrity.[33] This implies that adequate continuous treatment is indeed crucial for protection of the CNS.

Nonetheless, cART itself may cause damage to the CNS.[34] For example, efavirenz, a first-line treatment option for children older than 3 years, is strongly associated with relatively mild neurologic side effects such as bizarre dreams, but also—although rarely—with severe psychiatric symptoms such as depression or suicidal ideation.[35]

Despite being the largest MRI study in HIV-infected children using healthy, matched controls to date, this study is subject to several limitations. First, it is a cross-sectional assessment and cannot illustrate the course of the cerebral findings over time. A higher proportion of HIV-infected children were immigrants from sub-Saharan Africa, where the occurrence

Figure 2 Diffuse pattern of increased mean diffusivity in HIV-infected children compared to healthy controls

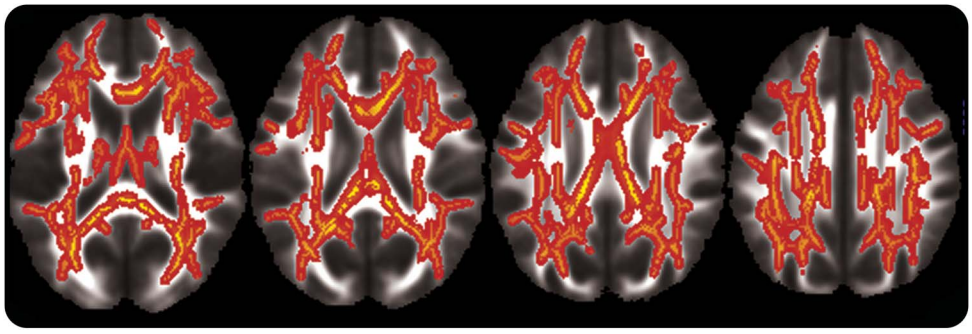

p Value < 0.05, threshold-free cluster enhancement–corrected. Significantly different voxels on the skeleton are projected on the average fractional anisotropy.

Table 3 Associations between HIV and cART-related factors and MRI outcome parameters in the HIV-infected group

		Total gray matter volume		Total white matter volume		White matter hyperintensities		Mean diffusivity		Fractional anisotropy	
	No.	Coefficient	*p* Value	Coefficient	*p* Value	Coefficient	*p* Value	Coefficient	*p* Value	Coefficient	*p* Value
HIV viral load zenith, log copies/mL	30	−27.52	0.053	−22.08	0.116	−0.91	0.115	0.38	0.657	−1.77	0.041[a]
Time HIV viral load detectable, y	34	−3.22	0.310	2.36	0.439	0.00	0.992	−0.29	0.091	−0.04	0.860
CD4 *Z* score nadir, SD	29	7.76	0.466	10.72	0.317	−0.29	0.341	−0.90	0.061	1.29	0.033[a]
Time CD4+ T-cells <500 × 10^6/L, m	34	−12.73	0.014[a]	−7.03	0.074	0.23	0.905	0.15	0.629	−0.66	0.067
Clinical marker											
CDC clinical category											
NA	10	—	—	—	—	—	—	—	—	—	—
B	16	−5.57	0.783	−48.42	0.006[a]	0.52	0.401	1.11	0.300	−1.79	0.167
C	8	5.12	0.823	−45.89	0.019[a]	0.10	0.890	1.27	0.314	−1.97	0.198
Therapy-related markers											
Age at start of cART, y	31	−2.84	0.338	3.22	0.249	0.16	0.065	0.03	0.837	0.05	0.740
Years without cART (% of life)	31	−0.22	0.535	0.63	0.051	0.02	0.099	0.00	0.906	0.01	0.606

Abbreviations: B = moderate symptoms; C = severe symptoms or AIDS; cART = combination antiretroviral therapy; CDC clinical category = Centers for Disease Control and Prevention clinical state at HIV diagnosis; NA = no to minimal symptoms.
Nadir = lowest CD4+ T-cell count; Zenith = highest HIV viral load.
All coefficients are adjusted for age and sex and the volumetric outcomes are additionally adjusted for intracranial volume.
[a] $p < 0.05$.

of malnutrition is high. Malnutrition early in life has been associated with cortical atrophy, and the higher proportion of immigrants may therefore have confounded the volumetric results.[36] In addition, the HIV-infected children were infected with a wide variety of HIV subtypes, including clade B and C. Differences in MRI-determined brain volumes have been found between adults with HIV-B and HIV-C infection,[37] and animal studies have postulated that HIV-C is less neuropathogenic than HIV-B.[38] We could not find significant associations between these HIV clades and MRI outcome parameters; however, this may be due to the small number of patients per subtype.

Also, more HIV-infected children were adopted or in foster care than controls. Possible unknown early-life circumstances such as maternal substance abuse, postnatal abuse, or neglect could have had a negative effect on cortical volume.[39,40] Finally, due to the relatively small sample size, associations between disease- and therapy-related factors, MRI results, and cognitive outcomes may have been incomplete.

Nonetheless, this study shows that HIV-infected children, of whom the majority were long-term virally suppressed with cART, have a lower GM and WM volume, a higher WM lesion load, and decreased WM integrity compared to controls. These differences occur in the context of poor cognitive performance in the HIV-infected group, and larger, longitudinal studies are needed to increase our understanding of the pathogenesis of cerebral injury in perinatally HIV-infected children.

AUTHOR CONTRIBUTIONS

Dr. Cohen recruited patients and controls, coordinated the study visits and performed the MRI scans, analyzed the data including statistical analysis, interpreted the results, and drafted the manuscript; she takes full responsibility for the data, the analyses and interpretation, and the conduct of the research, had full access to all of the data, and has the right to publish any and all data separate and apart from any sponsor. Dr. Caan designed the study, conceptualized the imaging protocol, supervised MRI scanning procedure and data analysis, interpreted the results, and revised the manuscript. Dr. Mutsaerts analyzed the data and revised the manuscript. Dr. Scherpbier recruited study patients and revised the manuscript. Prof. Dr. Kuijpers supervised study design and revised the manuscript. Prof. Dr. Reiss supervised study design, interpretation of results, and revised the manuscript. Prof. Dr. Majoie conceptualized the imaging protocol, supervised the MRI scanning procedure, analyzed the data, and revised the manuscript. Dr. Pajkrt designed the study, supervised study visits, interpreted the results, and revised the manuscript.

ACKNOWLEDGMENT

The authors thank Sandra van den Berg-Faaij for technical assistance; Geor Bakker for support with the TBSS analyses; Atie van der Plas and Annouschka Weijsenfeld for help in participant recruitment and data collection; and the parents and children participating in the study.

STUDY FUNDING

Supported by the Emma Foundation under grant number 11.001. This funding body had no role in the design or conduct of the study or in the analysis and interpretation of the results. Computations were performed using the e-bioinfra platform developed at the e-bioscience group of the Bioinformatics Laboratory of the AMC, using resources of the Dutch e-Science Grid, BiGGrid project, which is financially supported by the

Nederlandse Organisatie voor Wetenschappelijk Onderzoek (Netherlands Organisation for Scientific Research).

DISCLOSURE

The authors report no disclosures relevant to the manuscript. Go to Neurology.org for full disclosures.

Received December 24, 2014. Accepted in final form July 17, 2015.

REFERENCES

1. Laughton B, Cornell M, Boivin M, Van Rie A. Neurodevelopment in perinatally HIV-infected children: a concern for adolescence. J Int AIDS Soc 2013;16:18603.
2. Cardenas V, Meyerhoff DJ, Studholme C, et al. Evidence for ongoing brain injury in human immunodeficiency virus-positive patients treated with antiretroviral therapy. J Neurovirol 2009;15:324–333.
3. Ragin AB, Du H, Ochs R, et al. Structural brain alterations can be detected early in HIV infection. Neurology 2012;79:2328–2334.
4. Hoare J, Ransford GL, Philipps N, Amos T, Donald KA, Stein DJ. Systematic review of neuroimaging studies in vertically transmitted HIV positive children and adolescents. Metab Brain Dis 2014;29:221–229.
5. Johann-Liang R, Lin K, Cervia J, Stavola J, Noel G. Neuroimaging findings in children perinatally infected with the human immunodeficiency virus. Pediatr Infect Dis J 1998;17:753–754.
6. Sarma MK, Nagarajan R, Keller MA, et al. Regional brain gray and white matter changes in perinatally HIV-infected adolescents. Neuroimage Clin 2013;4:29–34.
7. Ackermann C, Andronikou S, Laughton B, et al. White matter signal abnormalities in children with suspected HIV-related neurologic disease on early combination antiretroviral therapy. Pediatr Infect Dis J 2014;66:207–212.
8. Hoare J, Fouche JP, Spottiswoode B, et al. A diffusion tensor imaging and neurocognitive study of HIV-positive children who are HAART-naïve "slow progressors." J Neurovirol 2012;18:205–212.
9. González-Scarano F, Martín-García J. The neuropathogenesis of AIDS. Nat Rev Immunol 2005;5:69–81.
10. Cohen S, ter Stege JA, Geurtsen GJ, et al. Poorer cognitive performance in perinatally HIV-infected children as compared to healthy socioeconomically matched controls. Clin Infect Dis 2015;1:1111–1119.
11. Christensen DL, Schieve LA, Devine O, Drews-Botsch C. Socioeconomic status, child enrichment factors, and cognitive performance among preschool-age children: results from the Follow-Up of Growth and Development Experiences study. Res Dev Disabil 2014;35:1789–1801.
12. Shahand S, Benabdelkader A, Jaghoori MM, et al. A data-centric neuroscience gateway: design, implementation, and experiences. Concurr Comput Pract Exp 2015;27:489–506.
13. Fischl B, Salat DH, Busa E, et al. Whole brain segmentation: neurotechnique automated labeling of neuroanatomical structures in the human brain. Neuron 2002; 33:341–355.
14. Caan MWA, Khedoe G, Poot D, et al. Adaptive noise filtering for accurate and precise diffusion estimation in fiber crossings. Med Image Comput Comput Assist Interv 2010;13:167–174.
15. Smith SM, Jenkinson M, Johansen-Berg H, et al. Tract-based spatial statistics: voxelwise analysis of multi-subject diffusion data. Neuroimage 2006;31:1487–1505.
16. Rueckert D, Sonoda LI, Hayes C, Hill DL, Leach MO, Hawkes DJ. Nonrigid registration using free-form deformations: application to breast MR images. IEEE Trans Med Imaging 1999;18:712–721.
17. Nichols TE, Holmes AP. Nonparametric permutation tests for functional neuroimaging: a primer with examples. Hum Brain Mapp 2002;15:1–25.
18. Mori S, Wakana S, Nagae-Poetscher LM, van Zijl PCM. MRI Atlas of Human White Matter. Amsterdam: Elsevier; 2005.
19. Fujishima M, Maikusa N, Nakamura K, Nakatsuka M, Matsuda H, Meguro K. Mild cognitive impairment, poor episodic memory, and late-life depression are associated with cerebral cortical thinning and increased white matter hyperintensities. Front Aging Neurosci 2014;6:306.
20. Iverson GL, Hakulinen U, Wäljas M, et al. To exclude or not to exclude: white matter hyperintensities in diffusion tensor imaging research. Brain Inj 2011;25: 1325–1332.
21. Di Perri C, Dwyer MG, Bergsland N, et al. White matter hyperintensities on 1.5 and 3 tesla brain MRI in healthy individuals. J Biomed Graph Comput 2013;3:53–62.
22. Schiffmann R, van der Knaap MS. Invited article: an MRI-based approach to the diagnosis of white matter disorders. Neurology 2009;72:750–759.
23. Nelson F, Datta S, Garcia N, et al. Intracortical lesions by 3T magnetic resonance imaging and correlation with cognitive impairment in multiple sclerosis. Mult Scler 2011; 17:1122–1129.
24. Lazeron RH, Langdon DW, Filippi M, et al. Neuropsychological impairment in multiple sclerosis patients: the role of (juxta)cortical lesion on FLAIR. Mult Scler 2000; 6:280–285.
25. Kim KW, MacFall JR, Payne ME. Classification of white matter lesions on magnetic resonance imaging in elderly persons. Biol Psychiatry 2008;64:273–280.
26. Hopkins RO, Beck CJ, Burnett DL, Weaver LK, Victoroff J, Bigler ED. Prevalence of white matter hyperintensities in a young healthy population. J Neuroimaging 2006;16:243–251.
27. Pillai JJ, Friedman L, Stuve TA, et al. Increased presence of white matter hyperintensities in adolescent patients with bipolar disorder. Psychiatry Res 2002;114:51–56.
28. Song SK, Sun SW, Ramsbottom MJ, Chang C, Russell J, Cross AH. Dysmyelination revealed through MRI as increased radial (but unchanged axial) diffusion of water. Neuroimage 2002;17:1429–1436.
29. Leite SCB, Corrêa DG, Doring TM, et al. Diffusion tensor MRI evaluation of the corona radiata, cingulate gyri, and corpus callosum in HIV patients. J Magn Reson Imaging 2013;38:1488–1493.
30. Hoare J, Jacqueline H, Westgarth-Taylor J, et al. A diffusion tensor imaging and neuropsychological study of prospective memory impairment in South African HIV positive individuals. Metab Brain Dis 2012;27:289–297.
31. Wright PW, Heaps JM, Shimony JS, Thomas JB, Ances BM. The effects of HIV and combination antiretroviral therapy on white matter integrity. AIDS 2012;26: 1501–1508.
32. Crowell CS, Malee KM, Yogev R, Muller WJ. Neurologic disease in HIV-infected children and the impact of combination antiretroviral therapy. Rev Med Virol 2014;24: 316–331.

33. Hoare J, Fouche J, Phillips N, et al. Clinical associations of white matter damage in cART-treated HIV-positive children in South Africa. J Neurovirol 2015;21:120–128.
34. Robertson K, Liner J, Meeker RB. Antiretroviral neurotoxicity. J Neurovirol 2013;18:388–399.
35. Mollan KR, Smurzynski M, Eron JJ, et al. Association between efavirenz as initial therapy for HIV-1 infection and increased risk for suicidal ideation or attempted or completed suicide: an analysis of trial data. Ann Intern Med 2014;161:1–10.
36. Potchen MJ, Kampondeni SD, Mallewa M, Taylor TE, Birbeck GL. Brain imaging in normal kids: a community-based MRI study in Malawian children. Trop Med Int Health 2013;18:398–402.
37. Ortega M, Heaps JM, Joska J, et al. HIV clades B and C are associated with reduced brain volumetrics. J Neurovirol 2013;19:479–487.
38. Rao VR, Sas AR, Eugenin EA, et al. HIV-1 clade-specific differences in the induction of neuropathogenesis. J Neurosci 2008;28:10010–10016.
39. Behnke M, Smith VC. Prenatal substance abuse: short- and long-term effects on the exposed fetus. Pediatrics 2013;131:1009–1024.
40. Van Harmelen AL, van Tol MJ, van der Wee NJA, et al. Reduced medial prefrontal cortex volume in adults reporting childhood emotional maltreatment. Biol Psychiatry 2010;68:832–838.

Cerebral injury in perinatally HIV-infected children compared to matched healthy controls

Sophie Cohen, Matthan W.A. Caan, Henk-Jan Mutsaerts, et al.

Neurology 2016;86;19-27 Published Online before print November 11, 2015
DOI 10.1212/WNL.0000000000002209